
Causal Graphs Underlying Generative Models: Path to Learning with Limited Data

Samuel C. Hoffman
IBM Research
shoffman@ibm.com

Kahini Wadhawan
IBM Research
kahini.wadhawan1@ibm.com

Payel Das
IBM Research
daspa@us.ibm.com

Prasanna Sattigeri
IBM Research
psattig@us.ibm.com

Karthikeyan Shanmugam
IBM Research*
karthikeyanvs@google.com

Abstract

Training generative models that capture rich semantics of the data and interpreting the latent representations encoded by such models are very important problems in unsupervised learning. In this work, we provide a simple algorithm that relies on perturbation experiments on latent codes of a pre-trained generative autoencoder to uncover a causal graph that is implied by the generative model. We leverage pre-trained attribute classifiers and perform perturbation experiments to check for influence of a given latent variable on a subset of attributes. Given this, we show that one can fit an effective causal graph that models a structural equation model between latent codes taken as exogenous variables and attributes taken as observed variables. One interesting aspect is that a single latent variable controls multiple overlapping subsets of attributes unlike conventional approach that tries to impose full independence. Using a pre-trained RNN-based generative autoencoder trained on a dataset of peptide sequences, we demonstrate that the learnt causal graph from our algorithm between various attributes and latent codes can be used to predict a specific property for sequences which are unseen. We compare prediction models trained on either all available attributes or only the ones in the Markov blanket and empirically show that in both the unsupervised and supervised regimes, typically, using the predictor that relies on Markov blanket attributes generalizes better for out-of-distribution sequences.

1 Introduction

While deep learning models demonstrate impressive performance in different prediction tasks, they often leverage correlations to learn a model of the data. As a result, accounting for the spurious ones among those correlations present in the data, which can correspond to biases, can weaken robustness of a predictive model on unseen domains with distributional shifts. Such failure can lead to serious consequences when deploying machine learning models in the real world.

Recently, there has been a plethora of work on the topic of causality in machine learning. A particular goal behind learning causal relations in data is to obtain better generalization across domains, the core idea being to decipher the causal mechanism that is invariant across domains of interest. Structural causal models have provided a principled framework for inferring causality from the data alone, which provides a better way to understand the data as well as the mechanisms underlying the generation of the data [1, 2]. In this framework, causal relationships among variables are represented with a

*currently at Google Research India.

Directed Acyclic Graph (DAG). However, learning structured causal models from observational data alone is possible for tabular data [3–5]. In many applications involving complex modalities, such as images, text, and biological sequencing data, it may not be reasonable to directly learn a causal graph on the observed covariates. For example, in the case of image data, the observed pixels may hide the structure of the causal generative factors [6]. Further in datasets with complex modalities, limited knowledge about meta data (additional attributes) of the datapoints may be available that can guide construction of such a causal model. Recent works like [7, 8] assume a causal structure (with no latent variables) amongst attributes in the meta data and they condition the generative model while training using this side information. Finally, for real-world applications with complex modalities it is critical to learn a “causal” model with limited labeled meta data. We focus on extracting a causal model between latent code of a generative model and attributes present in the meta-data (even if limited) leveraging the generative model trained on vast amounts of unsupervised data. Notably, since any accompanying metadata never exhaustively lists all causal generating factors of a data point (e.g. image), our procedure allows for unobserved latents between attributes in the meta data.

In this work, we propose a simple alternative to extract a “causal graph” relating different data attributes to latent representations learned by a given generative model trained on observational data. This generative model is pre-trained on large amount of unlabeled data. We then estimate the sensitivity of each of the data attributes by perturbing one latent dimension at a time, and use that sensitivity information to construct the causal graph of attributes. The model is finally tested by predicting an attribute on samples from a target distribution different from the source training data. Additionally, we are interested in scenarios where there is only limited data available from the target/test distribution.

To showcase the usefulness of the proposed framework, we focus on a scientific learning task: predicting the antimicrobial nature and/or activity of peptide sequences. This task is highly relevant in the context of the rising threat of antimicrobial resistance and lack of newer antibiotics [9]. Peptides with antimicrobial properties, that are part of innate immunity, are considered as the next generation of antibiotics. As a result, learning a data-driven model of antimicrobials is critical for identifying new peptides with antimicrobial properties. Antimicrobial peptides (AMP) can be active against different target species, and are expressed in different organisms. As a result, AMPs specifically active against a particular target species and/or originating from a certain host species can have different physico-chemical attributes, giving rise to remarkable structural and functional diversity [10–12]. This in turn gives rise to different AMP data distributions. As evaluating the antimicrobial property of a new peptide in a wet lab is costly and time-consuming, it is important to learn an antimicrobial predictor that generalizes well against all different AMP distributions, even when the distribution contains only a handful of datapoints, as is typically the case for newly evaluated or identified AMPs.

Below we list our contributions:

1. We propose a novel method to learn the causal structure between latent representations of a pre-trained generative model and attributes accompanying the dataset allowing for confounding between attributes.
2. We use the structure of the learnt model to do feature selection for predicting antimicrobial activities in out of distribution samples in a limited data setting.
3. Finally, we show that, the causal structure learned by our method, helps to achieve better generalization and is robust to distribution shifts.

2 Background and related work

Disentangled/Invariant Generative models: Several prior works [13–16] have considered learning generative models with a *disentangled* latent space. Many of them define disentanglement as the independence of the latent representation i.e., changing one dimension/factor of the latent representation does not affect others. Adversarial auto-encoder [14] and DIP-VAE [15] both achieve this by matching the *aggregated posterior* of the latent to the prior distribution. The former is trained as a deterministic auto-encoder and the latter as a variational auto-encoder. β -TCVAE [17] aims improved upon β -VAE [13] and achieves the independence directly using Total Correlation (TC) based loss. More generally, disentanglement requires that a primitive transformation in the observed data space (such as translation or rotation of images) results in a sparse change in the latent representation. In practice, the sparse changes can need not be *atomic* i.e., a change in the

observed space can lead to small but correlated latent factors. Additionally, it has been shown that it maybe impossible to achieve disentanglement without proper inductive biases or a form of supervision [18]. In [19], the authors use small number of ground truth latent factor labels and impose desired correlational structure to the latent space. Similarly, we extract a causal model between latent representations of the generative model and the attributes that are available in the form of metadata.

Discovering the causal structure of the latent factors is even more challenging but rewarding pursuit compared to discovering only the correlated latent factors as it allows us to ask causal questions such as the one arising from interventions or counterfactuals. Causal GAN [7] assumes that the the causal graph of the generative factors is known a priori and learns the functional relations by learning a good generative model. CausalVAE [20] shows that under certain assumptions, a linear structure causal model (SCM) on the latent space can be identified while training the generative model. In contrast, we learn the causal structure hidden in the pre-trained generative model in a post-hoc manner that does not affect the training of the generative model. This is similar to the work in [21], with the difference that our goal is to learn the causal structure in the latent space instead of the causal structure hidden in the decoder of the generative model.

Invariant Representation Learning Among conceptually related works, [22] focused on learning invariant correlations across multiple training distributions to explore causal structures underlying the data and allow OOD generalization. To achieve so, they proposed to find a representation ϕ such that the optimal classifier given ϕ is invariant across training environments. [23–25] proposed different training paradigms to train invariant classifiers.

Generative Models of Biological Sequences - In recent years, biological, in particular, protein/peptide sequence design has been approached using a diverse set of sequence-based deep generative models, including autoregressive language models, generative autoencoders, generative adversarial networks, and flow-based generators [26–36, 12]. Often, those generative models are coupled with search or sampling methods to enforce design of peptides with certain attributes. Inspired by the advances in text generation [37], many of those frameworks imposed structure in the latent space by semi-supervised training or discriminator learning with meta data/labels. Interestingly enough, representations learned by the generative models pre-trained on large volume of unlabeled data seem to capture important evolutionary, physico-chemical, and functional information about the peptides and show linear separation in term of attributes [30, 31]. A number of studies also have provided wet lab testing results of the machine-designed peptides, confirming the validity of the proposed designs [26, 30, 31].

Causality in Molecular Learning While machine learning models, including deep generative models, have been successful in deriving an informative representation of different classes of molecules including peptides, it remains non-trivial and largely unexplored to infer the relationship between different physico-chemical and functional attributes of the data. Though laws of chemistry and physics offer broad knowledge on that relationship, those are not enough to establish the causal mechanisms active in the system. For that reason, most experimental studies deal with partially known causal relationships, while confounding and observational bias factors (e.g. different experimental conditions such as temperature, assays, solution buffer) are abundant. In this direction, recently [38] have established the pairwise causal directions between a set of data descriptors of the microscopic images of molecular surfaces. Interestingly, they found that the causal relationships are consistent across a range of molecular composition. To our knowledge, this is the first work that infers a “causal” model between data attributes from the latents of a generative model of molecules (specifically peptides in this case) and shows the generalizability of the causal model across different data distributions.

3 Problem Setup and Methods

3.1 Problem Setup

Consider a generative model G that takes input latent code $z \in \mathbb{R}^{d \times 1}$ and generates a data point $x = G(z) \in \mathbb{R}^{p \times 1}$. We assume that it has been pre-trained using some training method (adversarial training, ELBO loss, etc.) on the data distribution $\mathbb{P}(x)$ sampled from the domain \mathcal{X} . We further have access to a vector of attributes $\mathbf{a}(x) \in \mathbb{R}^{|\mathcal{A}| \times 1}$ as meta data along with datapoints x . We assume



Figure 1: Example sparse weight matrix from a linear model trained on perturbation influences.

that we also have access to a pre-trained attribute classifiers (or estimators) from $p_{c_i}(\cdot) : \mathcal{X} \rightarrow \mathbb{R}$ producing a soft score/logit/regression estimate for the attribute $a_i(x)$.

The key problem we would like to solve is to find the structure of the causal model implied by the generative model and attribute classifier combination, where latent codes z act as the exogenous variables while $a_i(x)$ act as the observed variables. In other words, we hypothesize a structural causal model [1] as follows:

$$a_i(x) = f_i(\mathbf{a}_{\text{Pa}(i)}(x), z_{k_i}), \forall i \in [1 : |A|] \quad (1)$$

Here, $a_{\text{Pa}(i)}$ is a subset of the attributes $A = a_1(x) \dots a_{|A|}(x)$ that form the causal parents of $a_i(x)$. We can define a causal DAG $G(A, E)$ where $(i, j) \in E$ if $i \in \text{Pa}(j)$ in the structural causal model. Also, note that the ‘exogenous’ variables (e.g. $z_{k_i} \in \{z_1 \dots z_d\}$) are actually the latent representations/codes at the input of the Generator. We call this DAG the ‘structure of the causal model implied by the Generator’. Our principal aim is to learn a causal graph that is consistent with perturbation experiments on the latent codes z_i . In the structural causal model given by 1, we call z_{k_i} to be the latent variable associated with attribute $a_i(\cdot)$. Together the map from the space of latents z to $\mathbf{a}(x)$ can be called as the causal mechanism $\mathbf{a}(x) = M(z)$ as represented by structural causal model given by $\{f_1(\cdot) \dots f_{|A|}(\cdot)\}$.

3.2 Our Method - PerturbLearn

Our key idea is the following observation, if we take z_{k_i} associated with attribute $a_i(x)$, perturbing it to \tilde{z}_{k_i} would actually affect a_i and all its descendants in the causal graph. So we first obtain the sparse perturbation map between each latent z_j and the subset of attributes $A_j \subset A$ that it influences upon perturbation. Now, we apply a *peeling* algorithm that would actually find the attribute that is associated with a specific latent. In other words, we would find that attribute that occurs first in the causal order that is influenced by that latent variable. Our Algorithm 1 outputs a DAG with minimal edges that is consistent with the attribute sets for every latent variable. We assume that there is an encoding procedure $E(\cdot)$ that maps x to the corresponding z .

Perturbation Procedure: Given the pre-trained generative model G and a set of property predictors $a_i(\cdot)$, we: (i) Encode the sequence x into the latent code z through the encoder $E(\cdot)$, (ii) Choose any single dimension i in the latent space z and change z_i to \tilde{z}_i that is uniformly sampled in $[-B, B]$ (approximate range of the latent variables when encoded from the data points), (iii) Obtain $\tilde{x} = G(\tilde{z})$, (iv) Obtain the value of all attributes $\mathbf{a}(\tilde{x})$, and (v) Obtain the net influence vector $\Delta \mathbf{a}(x, \tilde{x}) = \mathbf{a}(x) - \mathbf{a}(\tilde{x})$. For attribute classifiers, we use the difference in logits while for continuous-valued attributes, we use the raw value. Each attribute is also standardized in order to scale the influences to similar ranges.

We then learn a sparse model with L1 regularization (Lasso) to predict the the latent change $z_i - \tilde{z}_i$ from the perturbations observed from the attributes $\Delta \mathbf{a}(x)$ for all data points x . This is repeated for every latent dimension i . We obtain a sparse weight matrix $W \in \mathbb{R}^{|A| \times |Z|}$ relating attributes in the rows to latent variables in the columns (see Figure 1 for one such example). If we pick the edges whose weights are above a specific threshold s , we obtain a sparse matrix. This would represent the attribute subsets each latent dimension influences. Now, we need to associate a latent to one or more attributes such that all attributes influenced by this latent appears later in the causal order.

Algorithm 1 PerturbLearn - Sparse weights to causal graph

Require: attributes A , latent features Z , weights $W \in \mathbb{R}^{|A| \times |Z|}$, sparsity $0 < s \leq 1$

- 1: **if** $|W_{i,j}| \leq s$ **then**
- 2: $W_{i,j} \leftarrow 0$ ▷ sparsify weights
- 3: **end if**
- 4: $X \leftarrow W$ ▷ working copy through diferent iterations
- 5: $G \leftarrow \text{DiGraph}$ ▷ empty graph
- 6: $C \leftarrow []$ ▷ empty list of confounded pairs of attributes
- 7: **while** X not empty **do**
- 8: $L \leftarrow 0^{|A| \times |Z|}$ ▷ Initialize with an $|A| \times |Z|$ all zero matrix.
- 9: $r_j \leftarrow \sum_i \mathbb{1}(X_{i,j} > 0)$ ▷ count number of attributes influenced by each latent feature
- 10: $j_{\min} \leftarrow \arg \min_j r_j$ ▷ start with latent features with minimal influence
- 11: $\forall j \in j_{\min}, L_{:,j} \leftarrow X_{:,j}$ ▷ Columns that correspond to latents with minimum influence
- forming leaves of the graph
- 12: **if** $\min_j r_j = 1$ **then**
- 13: **for** $i \in \text{rows}(L)$ **do** ▷ loop over rows (attributes)
- 14: $v \leftarrow \{j \in L_{i,j} \text{ if } \mathbb{1}(L_{i,j} > 0)\}$ ▷ latent variables that influence this attribute
- 15: $\text{succ} \leftarrow \{k : k \neq i, \mathbb{1}(W_{k,v} > 0)\}$ ▷ Other attribute nodes in the original graph, that were deleted and influenced by latent v
- 16: $G \leftarrow \text{node}(i)$ ▷ add node
- 17: $G \leftarrow \text{edge}(i, s) \quad \forall s \in \text{succ}$ ▷ add edges
- 18: **end for**
- 19: **else** ▷ hidden variable affects multiple properties
- 20: $S \leftarrow \emptyset$
- 21: **for** $j \in j_{\min}$ **do**
- 22: $S \leftarrow S + \{i : L_{i,j} > 0\}$
- 23: **end for**
- 24: $S \leftarrow \text{unique}(S)$ ▷ Select unique subsets of attributes that is affected by the latents with minimum influence.
- 25: **for** $I \in S$ **do** ▷ loop over unique sets of rows (confounded attributes)
- 26: $v \leftarrow \{j \in L_{i,j} \quad \forall i \in I \text{ if } \mathbb{1}(L_{i,j} > 0)\}$ ▷ latent variables that influence this attribute
- 27: $\text{succ} \leftarrow \{k : k \neq i, \mathbb{1}(W_{k,v} > 0)\}$ ▷ children
- 28: $G \leftarrow \text{node}(i) \quad \forall i \in I$ ▷ add node for each attribute
- 29: $C \leftarrow C + \text{permutations}(I, 2)$ ▷ Save all pairs of nodes in I as confounded nodes.
- 30: $G \leftarrow \text{edge}(i, s) \quad \forall i \in I, \forall s \in \text{succ}$ ▷ add edges
- 31: **end for**
- 32: **end if**
- 33: $X \leftarrow X_i \text{ if } L_i \notin L$ ▷ drop newly added attributes
- 34: $X \leftarrow X_j \quad \forall j \text{ if any}(\mathbb{1}(X_{i,j} > 0))$ ▷ drop corresponding channels
- 35: **end while**
- 36: $G \leftarrow \text{transitive_reduction}(G)$
- 37: $G \leftarrow \text{edge}(n, m) \quad \forall n, m \in C$
- 38: **return** G

Learning the DAG: Our proposed Algorithm PerturbLearn (Algorithm 1) learns the DAG iteratively starting from sink nodes. Suppose one could find a latent variable that influences only one attribute and suppose that the causal graph is a DAG, then that attribute should have no children. Therefore that node is added to the graph (and the corresponding latent is associated with it) (Lines 13 – 17 in Algorithm 1) and removed from the weight matrix (Lines 33 – 34 in Algorithm 1). Sometimes, during this recursion, there may be no latent variable that may be found to affect a single remaining attribute. We find a subset with smallest influence and add a confounding arrow between those attributes and add it to the graph (Lines 24 – 29). Now, if this latent affects any other downstream nodes previously removed, then we draw an edge from the current set of attributes to them (Lines 30). After the recursive procedure is performed, we obtain the transitive reduction [39] of the resulting DAG (Line 36). It is the minimal unique edge subgraph that preserves all ancestral relations. This would be the minimal causal model that would still preserve all latent-attribute influence relationships. See Figure 2 for a visualization of this process on a toy example.

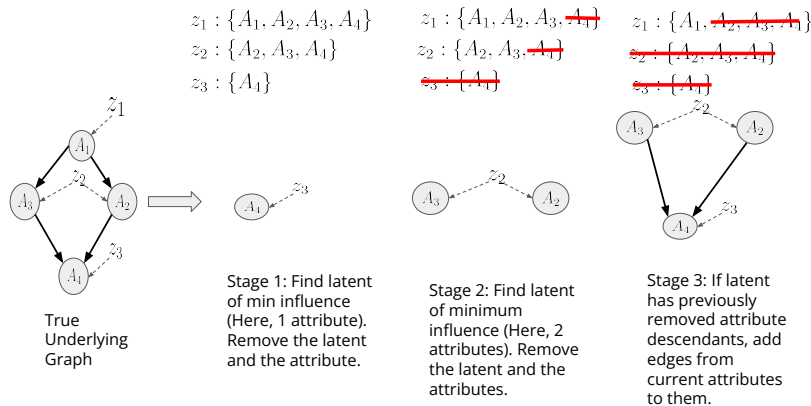


Figure 2: Illustrating various stages of PerturbLearn (Algorithm 1) using a toy underlying ground truth causal model.

Validating the Causal DAG on a Downstream Task We then investigate how the causal graph learned from the latent variables of a pre-trained autoencoder can help learn a predictor for an attribute from other attributes and possibly latent variables that can generalize on out-of-distribution (OOD) data. Suppose we want to predict the property $a_i(x)$, then using the DAG we actually look at the Markov Blanket of a_i , *i.e.* the set of attributes $MB(a_i) \subset A \cup Z$ which makes it independent of the rest of the variables. Usually, this is all parents, children, and co-parents in a causal DAG including any latent variables (which we know because we have access to z for every x).

The OOD prediction task considered here is antimicrobial potency regression. We consider antimicrobial peptides from different origins (expressed in different host such as animals, plants, bacteria, or synthetic), and use only one subset to learn a graph, as we assume that the graph holds true universally for any peptide — only the relative weights of each edge might change. We test the generality of the graph on AMPs active toward different classes of bacteria (Gram+ vs. Gram-) in two scenarios : a) semi-supervised with limited attribute data available in the target domain where we *retrain* only on the selected features from causal graph, b) unsupervised where we do not have access to attribute data in the target domain and directly *transfer* the learned causal graph and the functional relations between the nodes.

4 Data and Models

Datasets: For the experiments, we use a combination of data from various sources (Table 4). The majority comes from the DBAASP database [40]. For pre-processing the AMP sequences, we follow the procedure described in [30] with a maximum sequence length of 25 and sequences comprised of 20 natural amino acids only. We consider minimum inhibitory concentration (MIC) antimicrobial activity values, the source gene kingdom (organism), and target group(s), if available, from the database. The DBAASP new data partition consists of DBAASP sequences that were added after the publication of [30] and hence serve as an additional data source. We further consider the 32 machine-designed sequences that were tested in wet lab (AMP validated), as reported in [30], the 55 AMPs (human-AMP) identified in human proteome reported in [12], and 12 plant AMPs from PlantPepDB [41], as three additional data sources. When combining, we filtered duplicates by keeping the one with the minimum MIC.

Generative Autoencoder Details: The generative model was trained on peptide sequences comprised of 20 natural amino acids with a maximum length of 25. Specifically, 5000 AMP-labeled sequences from three AMP databases (DBAASP, satPDB and AMPEP) and 93k sequences from Uniprot-SwissProt and Uniprot-Trembl databases [42] were used. The autoencoder (AE) is comprised of an encoder-decoder pair, each comprised of a single-layer LSTM recurrent neural network [43]. In the typical VAE framework, a standard normal distribution is used as a prior of the latent code. A variational posterior $q(z|x)$ is then used to approximate the unknown true posterior $p(z|x)$. The

standard VAE objective consists of the sum of a reconstruction loss and a regularization constraint loss term: $L(\theta, \phi) = L_{rec}(\theta, \phi) + L_c(\phi)$, where the reconstruction loss is based on the negative log likelihood of the training sample, and the regularization $L_c(\phi)$ uses D_{KL} , the Kullback-Leibler divergence between the approximated posterior and the prior. To tackle the well-known “posterior collapse” experienced in the standard VAE training, many solutions have been proposed, such as KL annealing, adversarial training, or Wasserstein training. The pre-trained generative autoencoder used in this study was optimized using Wasserstein training, such that the marginal posterior $q_\phi(z) = E_x[q_\phi(z|x)]$ is constrained to be close to the prior $p(z)$, which is enforced by penalizing maximum mean discrepancy [44] with random features approximation of the radial basis function [45]: $L_c(\phi) = \text{MMD}(q_\phi(z), p(z))$. Details of the generative autoencoder architecture, training, and evaluation can be found in [30].

Sequence Attributes Table 6 lists a key set of physico-chemical properties governing peptide functions. We used monolithic binary classifiers trained directly on peptide sequences for predicting properties: AMP/non-AMP, toxic/non-toxic, broad/narrow-spectrum, helix/no structure and beta+helix/no structure from [30], with accuracy of 88%, 93.7%, 76%, 96%, 95.1%, respectively. For predicting the rest of the physico-chemical properties, the `GlobalDescriptor` and `GlobalAnalysis` classes from `modLAMP` [46] were used.

5 Results

In order to validate the causal graphs learned on the latent features of the generative autoencoder, we devise a series of experiments for learning with limited data. If the causal graph is valid, the Markov blanket of a given node should include all the features needed to predict that attribute and only those features. We hypothesize that this will lead to improved generalization and robustness when learning on only a few data points. We assume that the structure of the causal graph will not change when the domain shifts although the relative strength of causal links may change. However, these functions should be easy to learn given the minimal set of independent variables and therefore only a small dataset is needed.

To this end, we split the dataset according to biological kingdom of the source gene (or “Synthetic” if the peptide is not sourced from an organism) or by target bacterial group (Gram+ or Gram− only). Because the data is highly imbalanced toward positive examples and choosing a consistent threshold for binarizing the activity values is ambiguous, we choose a regression task. The task is to train a regressor to predict the lowest minimum inhibitory concentration (MIC) of a sequence reported against any target. There are two settings for this task: (i) retraining, where a new regressor is trained for each split using a small subset and tested on the remainder, and (ii) transfer, where a single regressor is trained on one split and tested on the others. For each choice of base split, we also learn the causal graph by perturbing that data. For each setting, we compare different sets of features on which to train the estimators: (i) (all props): a baseline of all the physico-chemical properties and functional properties used to learn the causal graph (except the AMP prediction), (ii) (blanket): just the attributes in the Markov blanket for AMP, (iii) (blanket+ z_{amp}): the Markov blanket attributes and the latent embedding features which directly influence the AMP node, and (iv) (z): the entire pre-trained latent embedding z .

Tables 1–3 show results of experiments on the regression task. The retraining setting uses a causal graph learned on the base split (first column — header italicized) peptides only and trains new regressors on $n_{\text{train}} = 10$ samples from each of the other splits for each different feature set. The regressor is then tested on the remainder of the data in that split and this is repeated $n = 100$ times to get the average performance. The transfer setting also uses the same causal graph but now trains a single regressor for each feature set on the full base split of peptides (minus a 10% held-out set). This regressor is then tested on the other full splits (except the training split which is tested on the held-out set). For example, in Table 1, the Synthetic-origin peptides are used to learn a causal graph and again when training the regression in the transfer setting.

We perform this regression task on the two domain splits (source organism and target group) for two different base splits each (Synthetic or Animalia and Gram+ or Gram−) and assess the performance using mean squared log error (MLSE). We also run each experiment for the following combination of hyperparameters: regressor model \in {linear regression (LR), random forest with 10 trees (RF), SVM

	n_{feat}	retrain				transfer			
		<i>Synth.</i>	<i>Anim.</i>	<i>Bact.</i>	<i>Plant.</i>	<i>Synth.</i>	<i>Anim.</i>	<i>Bact.</i>	<i>Plant.</i>
all props	17	3.354	2.492	2.377	3.280	2.649	5.650	9.654	4.530
blanket	8	3.265	2.373	2.360	3.486	2.543	5.810	8.286	3.942
blanket+ z_{amp}	5	3.255	2.415	2.311	3.243	2.595	1.962	2.653	3.349
z	100	3.321	2.434	2.392	3.356	2.462	1.931	2.440	3.669

Table 1: Regression results starting from Synthetic-origin peptides. Metric is mean squared log error (lower is better). Results for Synthetic-origin in the transfer case is on a held-out 10% test set. n_{feat} shows the dimensionality of each feature set. Best result for each column is shown in bold.

	n_{feat}	retrain				transfer			
		<i>Anim.</i>	<i>Synth.</i>	<i>Bact.</i>	<i>Plant.</i>	<i>Anim.</i>	<i>Synth.</i>	<i>Bact.</i>	<i>Plant.</i>
all props	17	2.390	3.349	2.310	3.403	2.105	4.299	6.271	2.855
blanket	3	2.485	3.228	2.385	3.184	2.102	2.844	2.185	4.162
blanket+ z_{amp}	3	2.409	3.335	2.379	3.277	2.083	2.907	2.119	4.245
z	100	2.340	3.194	2.379	3.303	1.983	4.617	6.422	2.763

Table 2: Regression results starting from Animalia-origin peptides. Metric is mean squared log error (lower is better). Results for Animalia-origin in the transfer case is on a held-out 10% test set. n_{feat} shows the dimensionality of each feature set. Best result for each column is shown in bold.

with RBF kernel}, Lasso sparsity parameter $\alpha \in \{0.0001, 0.0005, 0.001, 0.002\}$ and graph sparsity threshold $\delta \in \{0.1, 0.2, 0.25, 0.35\}$.

In order to determine the best combination of model type and causal graph to use for each experiment, we apply the following procedure:

- First, we look at only the test error of the transfer learning models on the base split held-out set. We choose the hyperparameters which produce the lowest error for each feature set. For all props and z , only the model type varies (LR/RF/SVM) while, for the feature sets which utilize causal information (blanket and blanket+ z_{amp}), there are additional sparsity hyperparameters.
- Using these models, we record the transfer performance on the remaining splits.
- Finally, we keep the graph constant from the best transfer learning model but now look at the test error of the retrained models on the base split. Again, we choose the model type which produces the lowest test error for each feature set.

In summary, we choose the best graph as the one which generalizes the best in transfer learning but independently choose the most robust model for each setting.

Table 1 shows the results of the experimental procedure above using Synthetic-origin peptides to learn the causal graph. For the retraining tasks, the blanket+ z_{amp} feature models outperform the all properties baseline. Blanket+ z_{amp} also outperforms all props by a significant margin in the transfer task, even though it is sometimes beaten by the z feature baseline. The number of features used is also much smaller (5 vs. 17 or 100) demonstrating that only a few of the features are necessary and sufficient. Additionally, while we see a performance drop from training on limited data in the retrain-Synthetic case compared to the base model in the transfer case, the models trained on only 10 samples outperform their transferred counterparts in many cases when comparing performance on the other splits, demonstrating the domain shift.

Table 2 shows similar results for the transfer task. Except for the Plantae split, the causal features perform better than the baseline. The results on the retraining setting are less clear: all four of the models perform about the same. Again, though, we see that the models which use causal information require many fewer features (only 3 each).

Table 3 shows the results of similar experiments as above, but this time the data split was based on the target bacteria group, Gram+ or Gram-. In both settings, the retrained regressor using the Markov

	n_{feat}	retrain		transfer		n_{feat}	retrain		transfer	
		<i>Gr.</i> +	<i>Gr.</i> -	<i>Gr.</i> +	<i>Gr.</i> -		<i>Gr.</i> -	<i>Gr.</i> +	<i>Gr.</i> -	<i>Gr.</i> +
all props	17	2.969	2.454	1.066	7.228	17	2.379	2.934	2.108	3.446
blanket	2	3.019	2.414	1.414	6.137	11	2.433	2.970	2.043	3.434
blanket+ z_{amp}	3	2.983	2.541	1.469	5.847	10	2.497	2.939	1.700	3.026
z	100	3.007	2.474	1.438	2.903	100	2.398	2.966	1.666	2.791

Table 3: Regression results starting from Gram+ (left) and Gram- (right) peptides. Metric is mean squared log error (lower is better). Results for each base split in the transfer case is on a held-out 10% test set. n_{feat} shows the dimensionality of each feature set. Best result for each column is shown in bold.

blanket alone or together with z_{amp} provides the best or on par performance on OOD data, when compared to all properties or the z -based model.

6 Discussion

One potential limitation of our framework is the dependency on a fixed set of data attributes, which may not be comprehensive. Further investigation on the accordance of the derived causal graph with domain priors and/or with expert knowledge would be addressed in future. We are not aware of any obvious negative impact of this work.

To conclude, in this study, we propose a framework to extract the causal graph relating different data attributes from the latents of a pre-trained generative model. The influence of a latent on attributes is used to construct the graph. Taken together, the results show the use of causal information (the Markov boundary alone or together with z_{amp}) improves over the all properties or all latents baseline. This is even true in the transfer case, demonstrating that the causal information leads to more robust and generalizable models.

References

- [1] J. Pearl, *Causality*. Cambridge university press, 2009.
- [2] S. Shimizu, P. O. Hoyer, A. Hyvärinen, A. Kerminen, and M. Jordan, “A linear non-gaussian acyclic model for causal discovery.” *Journal of Machine Learning Research*, vol. 7, no. 10, 2006.
- [3] M. Chickering, “Statistically efficient greedy equivalence search,” in *Conference on Uncertainty in Artificial Intelligence*. PMLR, 2020, pp. 241–249.
- [4] M. Kalisch and P. Bühlman, “Estimating high-dimensional directed acyclic graphs with the pc-algorithm.” *Journal of Machine Learning Research*, vol. 8, no. 3, 2007.
- [5] I. Tsamardinos, L. E. Brown, and C. F. Aliferis, “The max-min hill-climbing bayesian network structure learning algorithm,” *Machine learning*, vol. 65, no. 1, pp. 31–78, 2006.
- [6] K. Chalupka, P. Perona, and F. Eberhardt, “Visual causal feature learning,” *arXiv preprint arXiv:1412.2309*, 2014.
- [7] M. Kocaoglu, C. Snyder, A. G. Dimakis, and S. Vishwanath, “Causalgan: Learning causal implicit generative models with adversarial training,” *arXiv:1709.02023*, 2017.
- [8] H. Kim, S. Shin, J. Jang, K. Song, W. Joo, W. Kang, and I.-C. Moon, “Counterfactual fairness with disentangled causal effect variational autoencoder,” in *Proceedings of the AAAI Conference on Artificial Intelligence*, vol. 35, no. 9, 2021, pp. 8128–8136.
- [9] C. J. Murray, K. S. Ikuta, F. Sharara, L. Swetschinski, G. Robles Aguilar, A. Gray, C. Han, C. Bisignano, P. Rao, E. Wool, S. C. Johnson, A. J. Browne, M. G. Chipeta, F. Fell, S. Hackett, G. Haines-Woodhouse, B. H. Kashef Hamadani, E. A. P. Kumaran, B. McManigal,

- R. Agarwal, S. Akech, S. Albertson, J. Amuasi, J. Andrews, A. Aravkin, E. Ashley, F. Bailey, S. Baker, B. Basnyat, A. Bekker, R. Bender, A. Bethou, J. Bielicki, S. Boonkasidecha, J. Bukosia, C. Carvalheiro, C. Castañeda-Orjuela, V. Chansamouth, S. Chaurasia, S. Chiurchiù, F. Chowdhury, A. J. Cook, B. Cooper, T. R. Cressey, E. Criollo-Mora, M. Cunningham, S. Darboe, N. P. J. Day, M. De Luca, K. Dokova, A. Dramowski, S. J. Dunachie, T. Eckmanns, D. Eibach, A. Emami, N. Feasey, N. Fisher-Pearson, K. Forrest, D. Garrett, P. Gastmeier, A. Z. Giref, R. C. Greer, V. Gupta, S. Haller, A. Haselbeck, S. I. Hay, M. Holm, S. Hopkins, K. C. Iregbu, J. Jacobs, D. Jarovsky, F. Javanmardi, M. Khorana, N. Kissoon, E. Kobeissi, T. Kostyanov, F. Krapp, R. Krumkamp, A. Kumar, H. H. Kyu, C. Lim, D. Limmathurotsakul, M. J. Loftus, M. Lunn, J. Ma, N. Mturi, T. Munera-Huertas, P. Musicha, M. M. Mussi-Pinhata, T. Nakamura, R. Nanavati, S. Nangia, P. Newton, C. Ngoun, A. Novotney, D. Nwakanma, C. W. Obiero, A. Olivas-Martinez, P. Olliaro, E. Ooko, E. Ortiz-Brizuela, A. Y. Peleg, C. Perrone, N. Plakkal, A. P. de Leon, M. Raad, T. Ramdin, A. Riddell, T. Roberts, J. V. Robotham, A. Roca, K. E. Rudd, N. Russell, J. Schnall, J. A. G. Scott, M. Shivamallappa, J. Sifuentes-Osornio, N. Steenkeste, A. J. Stewardson, T. Stoeva, N. Tasak, A. Thaiprakong, G. Thwaites, C. Turner, P. Turner, H. R. van Doorn, S. Velaphi, A. Vongpradith, H. Vu, T. Walsh, S. Waner, T. Wangrangsimakul, T. Wozniak, P. Zheng, B. Sartorius, A. D. Lopez, A. Stergachis, C. Moore, C. Dolecek, and M. Naghavi, “Global burden of bacterial antimicrobial resistance in 2019: a systematic analysis,” *The Lancet*, 2022. [Online]. Available: <https://www.sciencedirect.com/science/article/pii/S0140673621027240>
- [10] E. F. Haney, S. K. Straus, and R. E. Hancock, “Reassessing the host defense peptide landscape,” *Frontiers in chemistry*, vol. 7, p. 43, 2019.
- [11] M. A. Hanson, A. Dostálová, C. Ceroni, M. Poidevin, S. Kondo, and B. Lemaitre, “Synergy and remarkable specificity of antimicrobial peptides in vivo using a systematic knockout approach,” *Elife*, vol. 8, p. e44341, 2019.
- [12] M. Jain, E. Bengio, A.-H. Garcia, J. Rector-Brooks, B. F. Dossou, C. Ekbote, J. Fu, T. Zhang, M. Kilgour, D. Zhang *et al.*, “Biological sequence design with gflownets,” *arXiv preprint arXiv:2203.04115*, 2022.
- [13] I. Higgins, L. Matthey, A. Pal, C. Burgess, X. Glorot, M. Botvinick, S. Mohamed, and A. Lerchner, “beta-vae: Learning basic visual concepts with a constrained variational framework,” in *International Conference on Learning Representations*, 2017.
- [14] A. Makhzani, J. Shlens, N. Jaitly, I. Goodfellow, and B. Frey, “Adversarial autoencoders,” *arXiv preprint arXiv:1511.05644*, 2015.
- [15] A. Kumar, P. Sattigeri, and A. Balakrishnan, “Variational inference of disentangled latent concepts from unlabeled observations,” *arXiv:1711.00848*, 2017.
- [16] H. Kim and A. Mnih, “Disentangling by factorising,” in *International Conference on Machine Learning*. PMLR, 2018, pp. 2649–2658.
- [17] R. T. Chen, X. Li, R. B. Grosse, and D. K. Duvenaud, “Isolating sources of disentanglement in variational autoencoders,” *Advances in neural information processing systems*, vol. 31, 2018.
- [18] F. Locatello, S. Bauer, M. Lucic, G. Raetsch, S. Gelly, B. Schölkopf, and O. Bachem, “Challenging common assumptions in the unsupervised learning of disentangled representations,” in *international conference on machine learning*. PMLR, 2019, pp. 4114–4124.
- [19] F. Träuble, E. Creager, N. Kilbertus, F. Locatello, A. Dittadi, A. Goyal, B. Schölkopf, and S. Bauer, “On disentangled representations learned from correlated data,” in *International Conference on Machine Learning*. PMLR, 2021, pp. 10 401–10 412.
- [20] M. Yang, F. Liu, Z. Chen, X. Shen, J. Hao, and J. Wang, “Causalvae: Disentangled representation learning via neural structural causal models,” in *Proceedings of the IEEE/CVF Conference on Computer Vision and Pattern Recognition*, 2021, pp. 9593–9602.
- [21] M. Besserve, R. Sun, and B. Schoelkopf, “Tinkering with black boxes: counterfactuals uncover modularity in generative models,” 2018.

- [22] M. Arjovsky, L. Bottou, I. Gulrajani, and D. Lopez-Paz, “Invariant risk minimization,” *arXiv preprint arXiv:1907.02893*, 2019.
- [23] K. Ahuja, K. Shanmugam, K. Varshney, and A. Dhurandhar, “Invariant risk minimization games,” in *International Conference on Machine Learning*. PMLR, 2020, pp. 145–155.
- [24] C. Lu, Y. Wu, J. M. Hernández-Lobato, and B. Schölkopf, “Nonlinear invariant risk minimization: A causal approach,” *arXiv preprint arXiv:2102.12353*, 2021.
- [25] A. Robey, G. J. Pappas, and H. Hassani, “Model-based domain generalization,” *Advances in Neural Information Processing Systems*, vol. 34, pp. 20 210–20 229, 2021.
- [26] D. Nagarajan, T. Nagarajan, N. Roy, O. Kulkarni, S. Ravichandran, M. Mishra, D. Chakravorty, and N. Chandra, “Computational antimicrobial peptide design and evaluation against multidrug-resistant clinical isolates of bacteria,” *Journal of Biological Chemistry*, pp. jbc–M117, 2017.
- [27] P. Das, K. Wadhawan, O. Chang, T. Sercu, C. D. Santos, M. Riemer, V. Chenthamarakshan, I. Padhi, and A. Mojsilovic, “Pepcvae: Semi-supervised targeted design of antimicrobial peptide sequences,” *arXiv preprint arXiv:1810.07743*, 2018.
- [28] D. H. Brookes, H. Park, and J. Listgarten, “Conditioning by adaptive sampling for robust design,” in *ICML*, 2019.
- [29] A. Kumar and S. Levine, “Model inversion networks for model-based optimization,” in *Advances in Neural Information Processing Systems*, H. Larochelle, M. Ranzato, R. Hadsell, M. F. Balcan, and H. Lin, Eds., vol. 33. Curran Associates, Inc., 2020, pp. 5126–5137. [Online]. Available: <https://proceedings.neurips.cc/paper/2020/file/373e4c5d8edfa8b74fd4b6791d0cf6dc-Paper.pdf>
- [30] P. Das, T. Sercu, K. Wadhawan, I. Padhi, S. Gehrmann, F. Cipcigan, V. Chenthamarakshan, H. Strobel, C. Dos Santos, P.-Y. Chen *et al.*, “Accelerated antimicrobial discovery via deep generative models and molecular dynamics simulations,” *Nature Biomedical Engineering*, vol. 5, no. 6, pp. 613–623, 2021.
- [31] J.-E. Shin, A. J. Riesselman, A. W. Kollasch, C. McMahon, E. Simon, C. Sander, A. Manglik, A. C. Kruse, and D. S. Marks, “Protein design and variant prediction using autoregressive generative models,” *Nature communications*, vol. 12, no. 1, pp. 1–11, 2021.
- [32] S. C. Hoffman, V. Chenthamarakshan, K. Wadhawan, P.-Y. Chen, and P. Das, “Optimizing molecules using efficient queries from property evaluations,” *Nature Machine Intelligence*, pp. 1–11, 2021.
- [33] A. Tucs, D. P. Tran, A. Yumoto, Y. Ito, T. Uzawa, and K. Tsuda, “Generating ampicillin-level antimicrobial peptides with activity-aware generative adversarial networks,” *ACS omega*, vol. 5, no. 36, pp. 22 847–22 851, 2020.
- [34] Y. Cao, P. Das, V. Chenthamarakshan, P.-Y. Chen, I. Melnyk, and Y. Shen, “Fold2seq: A joint sequence(1d)-fold(3d) embedding-based generative model for protein design,” in *Proceedings of the 38th International Conference on Machine Learning*, ser. Proceedings of Machine Learning Research, M. Meila and T. Zhang, Eds., vol. 139. PMLR, 18–24 Jul 2021, pp. 1261–1271. [Online]. Available: <https://proceedings.mlr.press/v139/cao21a.html>
- [35] D. Repecka, V. Jauniskis, L. Karpus, E. Rembeza, I. Rokaitis, J. Zrimec, S. Poviloniene, A. Laurynenas, S. Viknander, W. Abuajwa *et al.*, “Expanding functional protein sequence spaces using generative adversarial networks,” *Nature Machine Intelligence*, vol. 3, no. 4, pp. 324–333, 2021.
- [36] S. R. Johnson, S. Monaco, K. Massie, and Z. Syed, “Generating novel protein sequences using gibbs sampling of masked language models,” *bioRxiv*, 2021.
- [37] Z. Hu, Z. Yang, X. Liang, R. Salakhutdinov, and E. P. Xing, “Toward controlled generation of text,” in *International Conference on Machine Learning*, 2017, pp. 1587–1596.

- [38] M. Ziatdinov, C. T. Nelson, X. Zhang, R. K. Vasudevan, E. Eliseev, A. N. Morozovska, I. Takeuchi, and S. V. Kalinin, “Causal analysis of competing atomistic mechanisms in ferroelectric materials from high-resolution scanning transmission electron microscopy data,” *npj Computational Materials*, vol. 6, no. 1, pp. 1–9, 2020.
- [39] A. V. Aho, M. R. Garey, and J. D. Ullman, “The transitive reduction of a directed graph,” *SIAM Journal on Computing*, vol. 1, no. 2, pp. 131–137, 1972.
- [40] M. Pirtskhalava, A. Gabrielian, P. Cruz, H. L. Griggs, R. B. Squires, D. E. Hurt, M. Grigolava, M. Chubinidze, G. Gogoladze, B. Vishnepolsky *et al.*, “Dbaasp v. 2: an enhanced database of structure and antimicrobial/cytotoxic activity of natural and synthetic peptides,” *Nucleic acids research*, vol. 44, no. D1, pp. D1104–D1112, 2016.
- [41] D. Das, M. Jaiswal, F. N. Khan, S. Ahamad, and S. Kumar, “Plantpepdb: A manually curated plant peptide database,” *Scientific reports*, vol. 10, no. 1, pp. 1–8, 2020.
- [42] P. EMBL-EBI, SIB, “Universal Protein Resource (UniProt),” <https://www.uniprot.org>, 2018, [Online; accessed August-2018].
- [43] S. Hochreiter and J. Schmidhuber, “Long short-term memory,” *Neural computation*, vol. 9, no. 8, pp. 1735–1780, 1997.
- [44] A. Gretton, K. M. Borgwardt, M. Rasch, B. Schölkopf, and A. J. Smola, “A kernel method for the two-sample-problem,” in *Advances in neural information processing systems*, 2007, pp. 513–520.
- [45] A. Rahimi and B. Recht, “Random features for large-scale kernel machines,” in *Advances in neural information processing systems*, 2007, pp. 1177–1184.
- [46] A. T. Müller, G. Gabernet, J. A. Hiss, and G. Schneider, “modlamp: Python for antimicrobial peptides,” *Bioinformatics*, vol. 33, no. 17, pp. 2753–2755, 2017.
- [47] M. D. Torres, M. C. Melo, O. Crescenzi, E. Notomista, and C. de la Fuente-Nunez, “Mining for encrypted peptide antibiotics in the human proteome,” *Nature Biomedical Engineering*, vol. 6, no. 1, pp. 67–75, 2022.
- [48] D. M. Chickering, “Optimal structure identification with greedy search,” *Journal of machine learning research*, vol. 3, no. Nov, pp. 507–554, 2002.
- [49] J. Friedman, T. Hastie, and R. Tibshirani, “Sparse inverse covariance estimation with the graphical lasso,” *Biostatistics*, vol. 9, no. 3, pp. 432–441, 2008.
- [50] A. A. Margolin, I. Nemenman, K. Basso, C. Wiggins, G. Stolovitzky, R. Dalla Favera, and A. Califano, “Aracne: an algorithm for the reconstruction of gene regulatory networks in a mammalian cellular context,” in *BMC bioinformatics*, vol. 7, no. 1. BioMed Central, 2006, pp. 1–15.
- [51] D. Kalainathan and O. Goudet, “Causal discovery toolbox: Uncover causal relationships in python,” 2019. [Online]. Available: <https://arxiv.org/abs/1903.02278>

Appendix

A Data and Pre-trained Property Estimators and Predictors

name	source	size	% pos.	description
DBAASP	[30]	4626	61%	DBAASP (pre-2021)
AMP validated	[30]	32	69%	Machine-designed and experimentally validated
DBAASP new		4331	71%	DBAASP (post-2021)
Human AMP*	[47]	55	72%	AMP-positive only
Plant AMP	[41]	12	50%	PlantPepDB

Table 4: Overview of datasets used. Binary threshold of AMP activity: 128 $\mu\text{g}/\text{mL}$. *Human AMPs were obtained through personal communications with authors of [12].

kingdom/target	size	% pos.
Synthetic	4010	85
Animalia	682	89
Bacteria	35	91
Plantae	26	65
Gram+	242	–
Gram–	465	–

Table 5: Combined dataset broken down by source or target after filtering for length ≤ 25 . Binary threshold of AMP activity: 128 $\mu\text{g}/\text{mL}$.

name	source	description
Length	modlamp.descriptors.GlobalDescriptor	sequence length (AA count)
MW	modlamp.descriptors.GlobalDescriptor	molecular weight
Charge	modlamp.descriptors.GlobalDescriptor	overall charge
ChargeDensity	modlamp.descriptors.GlobalDescriptor	charge / MW
pI	modlamp.descriptors.GlobalDescriptor	isoelectric point
InstabilityInd	modlamp.descriptors.GlobalDescriptor	protein stability
Aromaticity	modlamp.descriptors.GlobalDescriptor	relative frequency of Phe+Trp+Tyr
AliphaticInd	modlamp.descriptors.GlobalDescriptor	thermal stability
BomanInd	modlamp.descriptors.GlobalDescriptor	protein-protein interaction
HydrophRatio	modlamp.descriptors.GlobalDescriptor	relative frequency of the amino acids A,C,F,I,L,M & V
Hydrophobicity	modlamp.analysis.GlobalAnalysis	measures AA residues interaction compatibility with lipid bilayer
HydrophobicMoment	modlamp.analysis.GlobalAnalysis	measure of amphiphilicity \perp to the axis of periodic peptide structure
amp	pre-trained sequence classifier [30]	antimicrobial (binary)
tox	pre-trained sequence classifier [30]	toxicity (binary)
broad	pre-trained sequence classifier [30]	broad spectrum (binary)
helix	pre-trained sequence classifier [30]	helix structure (binary)
helix_beta	pre-trained sequence classifier [30]	beta + helix structure (binary)

Table 6: Attributes used as nodes in the causal graph.

Attribute	Data-Split			Accuracy (%)		Screening
	Train	Valid	Test	Majority Class	Test	Threshold
AMP	6489	811	812	68.9	88.0	7.944
Toxic	8153	1019	1020	82.73	93.7	-1.573
Broad spectrum	2031	254	255	51.37	76.0	-7.323
Structure (beta helix)	2644	331	331	64.65	95.1	-5.382

Table 7: Performance of sequence-based LSTM classifiers on different attributes. Adapted from reference [30].

B Additional Methods Details: Code Snippet

```

1 def learn_graph(df, sparsity):
2     df[abs(df) < sparsity] = None
3     df = df.dropna(axis=1, how='all')
4     df_orig = df.copy()
5
6     G = nx.DiGraph()
7     confounded = []
8     while not df.empty:
9         ct = df.count()
10        leaf_cs = ct.index[ct == ct.min()]
11        leaf_df = df.loc[:, leaf_cs].dropna(axis=0, how='all')
12        if ct.min() == 1:
13            for attr in leaf_df.index:
14                channels = leaf_df.loc[attr].dropna().index.tolist()
15                G.add_node(attr, channels=channels)
16                children = df_orig.loc[:, channels].drop(attr).dropna(axis=0, how='all').index.tolist()
17                G.add_edges_from(product([attr], children))
18        else:
19            subsets = leaf_df.apply(lambda c: tuple(c.notna()))
20            for s in subsets.unique():
21                ldf = leaf_df.loc[:, subsets[subsets == s].index].dropna(axis=0, how='all')
22                attrs = ldf.index.tolist()
23                channels = ldf.columns.tolist()
24                G.add_nodes_from(set(attrs) - set(G.nodes))
25                children = df_orig.loc[:, channels].drop(attrs).dropna(axis=0, how='all').index.tolist()
26                # adds cycles; wait until after transitive_reduction to add:
27                confounded.extend(permutations(attrs, 2))
28                G.add_edges_from(product(attrs, children))
29        df = df.drop(leaf_df.index)
30        df = df.dropna(axis=1, how='all')
31
32    G = nx.transitive_reduction(G)
33    G.add_edges_from(confounded)
34    return G

```

Figure 3: Code corresponding to Algorithm 1

C Compute Details

We ran the experiments on a cluster of nodes using CPUs only (Intel Xeon E5 v4 family processors). The perturbation procedure took around 90 minutes to complete but only needed to be done once per split (e.g. Synthetic, Gram+) which could be done in parallel. Deriving the causal graph and learning regressors took only minutes and hyperparameter configurations could be run in parallel.

D Additional Results

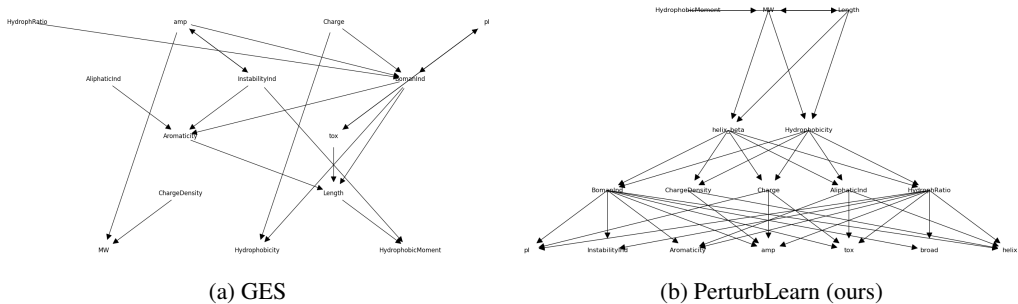


Figure 4: Comparison of causal graph generated using (a) the Greedy Equivalence Search (GES) algorithm and (b) PerturbLearn, our method ($\alpha = 0.002$, $\delta = 0.1$). Note: GES shows the Markov equivalence class where bidirectional arrows imply one or the other direction may be true (for PerturbLearn, bidirectional arrows mean the nodes are confounded). Also, GES does not include broad, helix, or helix_beta nodes because we did not have access to those labels for this dataset. The PerturbLearn graph shown was used in the blanket+ z_{amp} row of Table 1.

We compare a graph generated via a well-known causal discovery method, Greedy Equivalence Search (GES) [48]. In order to run the GES algorithm, we compile a dataset with ground-truth labels for all properties. This means we need labels for each sequence even though the classifiers for each property were trained independently and may have used non-overlapping datasets. Therefore, the data we used included AMP and toxicity labels but not broad spectrum or structure (helix/beta+helix) labels. The size of this dataset was 4798. We first run Graph Lasso [49] to get a skeleton graph and then remove indirect links using the Aracne algorithm [50]. Finally, we run the GES algorithm with the labeled data and skeleton. We ran this analysis using the Causal Discovery Toolbox [51].

Comparing the graph from GES and the one from PerturbLearn, the GES graph seems to defy intuition more. For example, the AMP property is not caused by any other property (except possible InstabilityInd) while length is “caused” by toxicity, among other properties. PerturbLearn generally maintains a hierarchy from basic features like length and MW at the top to more complex properties like AMP and toxicity at the bottom.